KAWASAKI STEEL TECHNICAL REPORT
No.22 (May 1990)
Advanced Technologies of Iron and Steel,
Commemorating the 20th Anniversary
of the Technical Research Division

Thin Film X-Ray Diffraction Method Using Vacuum Pass Line

Michio Katayama, Masato Shimizu, Tizuko Maeda

Synopsis :
A new type of X-ray diffractometer for ultra-thin-film, applicable in vacuum, has been developed. This analysis method has made it possible to increase peak intensity of diffraction measured in vacuum in comparison with in air, resulting in successful detection of an ultra-thin film less than 10 nm in thickness. Its application to the surface film analysis revealed that (1) the thickness of FeCr2O4 film formed on AISI 304 stainless steel during bright annealing increased rapidly when the dew point exceeded -40℃, and (2) crystallization temperature of amorphous metal of the Fe-B-Si system depended upon the annealing atmosphere and crystallization started at the surface.

The body can be viewed from the next page.

Thin Film X-Ray Diffraction Method Using Vacuum Pass Line*

Michio Katayama
Senior Researcher, Instrumentation & Analytical Science Research Center

Masato Shimizu
Dr. Engi., Senior Researcher, Instrumentation & Analytical Science Research Center

Tizuko Maeda
Researcher, Instrumentation & Analytical Science Research Center

Synopsis:

A new type of X-ray diffractometer for ultra-thin-film, applicable in vacuum, has been developed. This analysis method has made it possible to increase peak intensity of diffraction measured in vacuum in comparison with in air, resulting in successful detection of an ultra-thin film less than 10 nm in thickness. Its application to the surface film analysis revealed that (1) the thickness of $FeCr_2O_4$ film formed on AISI 304 stainless steel during bright annealing increased rapidly when the dew point exceeded −40°C, and (2) crystallization temperature of amorphous metal of the Fe–B–Si system depended upon the annealing atmosphere and crystallization started at the surface.

1 Introduction

A notable trend in recent years is a development of new materials with their properties improved over their conventional levels through a reconstitution of surface properties. This is achieved by a film formed electrically, chemically or physically over a metallic material using a substance different from the metallic substrate.

The θ-2θ scanning X-ray diffraction method has long been used to clarify the crystal structure of substances as one of the most familiar techniques for evaluating the properties of materials, under which however, it is difficult to detect diffracted X-rays reflected from film of several tens of nanometer, making it impossible to clarify the structure.

Kawasaki Steel has recently developed an X-ray diffractometer which is provided with a vacuum pass line based on the grazing incidence method for application to the structural analysis of thin coating films.[1-4] This paper presents the principle, makeup and features of the apparatus, and describes examples of its application to steel materials.

2 Principle and Makeup

2.1 Thin Film X-Ray Diffraction (TFXD) Method

Sufficiently thick samples are measured with conventional Bragg-Brentano diffractometers. Parafocusing geometry is used to obtain high resolution of angle and intensity; in general, the θ-2θ method is adopted which involves measuring of the crystal lattice planes existing parallel to the surface of the specimen. In this apparatus, however, the incident X-ray beam is caused to strike on the surface of the specimen at a low angle to minimize the penetration of X-rays, as shown in **Fig. 1**. With the incident X-ray beam and specimen kept fixed, the receiving slit, crystal monochrometer and X-ray detector work in unison to perform angle scanning with the specimen axis serving as the center.

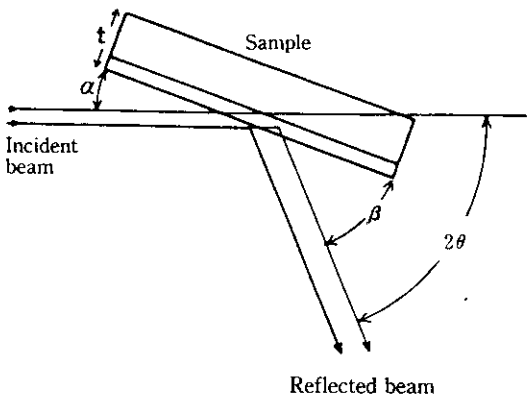

Fig. 1 Surface reflection

* Originally published in *Kawasaki Steel Giho*, 21(1989)2, pp. 77–82

2.2 Diffraction X-Ray Intensity and Penetration Depth

Diffraction X-ray intensities (I_r) obtained in the TFXD method are calculated by Eq. (1) by giving the linear absorption coefficient of the substance, film thickness, incident angle, and reflection angle.[5,6]

$$I_r = \frac{I_0 S(\sin\beta)\{1 - \exp[-\mu t(\mathrm{cosec}\,\alpha + \mathrm{cosec}\,\beta)]\}}{\mu(\sin\alpha + \sin\beta)} \cdots(1)$$

where I_0: Diffraction X-ray intensity per unit volume without absorption
S: Sectional area of incident X-ray beam flux
α: Angle formed between specimen and incident X-ray beam
β: Angle formed between specimen and X-ray detector
μ: Linear absorption coefficient of specimen
t: Thickness of specimen

Figure 2 shows the dependence of incident angle on the diffraction X-ray intensity for a 100-nm thick specimen. As is apparent from this figure, under the θ-2θ method, the diffraction X-ray intensity decreases abruptly with increasing diffraction angle. On the other hand, the diffraction X-ray intensity increases as the incident angle (α) decreases. In measuring a thin film, it is effective to set α at as low an angle as possible, although it depends on the surface condition of the specimen.

Next, the effective penetration depth (t) is calculated by Eq. (2) from the diffraction X-ray intensity ratio of the thickness of a sufficiently thick specimen to a finite thickness.[7]

$$R_x = \int_{t=0}^{t=t} d\,\mathrm{ID} \Big/ \int_{t=0}^{t=\infty} d\,\mathrm{ID}$$

$$= 1 - \exp\{-\mu t(1/\sin\alpha + 1/\sin\beta)\} \cdots(2)$$

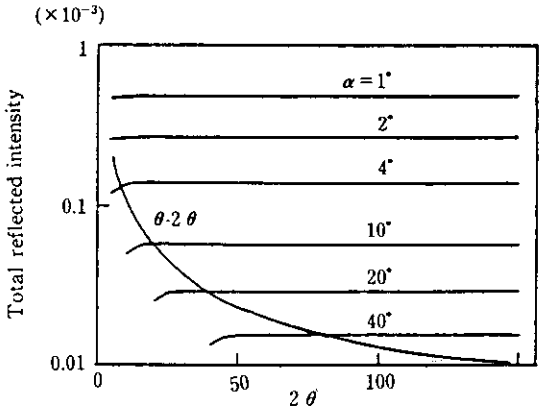

Fig. 2 X-ray reflected intensity for thin specimen (t = 100 nm)

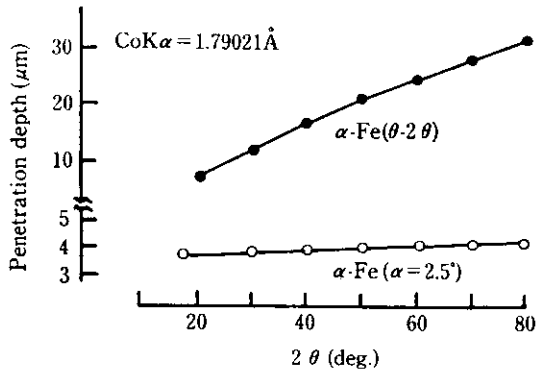

Fig. 3 Effective penetration depth changes with incident angles by the θ-2θ diffraction method and TFXD (α = 2.5)

where R_x: Diffraction X-ray intensity ratio obtained from a sufficiently thick specimen and a thin film
ID: X-ray intensity per unit area
μ: Linear absorption coefficient
t: Penetration depth
α: Angle formed between specimen and incident X-ray beam
β: Angle formed between specimen and X-ray detector

Since α is constant for the TFXD method, t is given by Eq. (3):

$$t = \frac{-\ln(1 - R_x)\sin\alpha\sin\beta}{\mu(\sin\alpha + \sin\beta)} \cdots\cdots(3)$$

Figure 3 shows the difference in the penetration depth between the θ-2θ method and the TFXD method for R_x of 0.99 ($K_x = 4.61$). The calculation reveals that the penetration depths for the θ-2θ diffraction method are twice to eight times those of TFXD. Therefore, the θ-2θ diffraction method has greater dependence on the diffraction angle (2θ).

As is naturally presumed, the penetration depth depends on the wavelength of X-ray and specimen. **Figure 4** shows K-absorption edges and mass absorption coefficients of several substances and the wavelengths of characteristic X-rays of X-ray sources. When the substance that composes a thin film is Fe, NiKα is desirable; however, CuKα does not produce a great difference. In the case of Cr, it is appropriate to use FeKα; CrKα is desirable for Ti. In the case of Ga and Si, the penetration depth can be reduced by using characteristic X-rays of long wavelength. The same applies to other specific substances, i.e., Ti and other elements with atomic number lower than 22 as well as Cu and other elements with atomic number higher than 29. It is improper to use X-rays of short wavelength, such as MoKα, for measuring thin films.

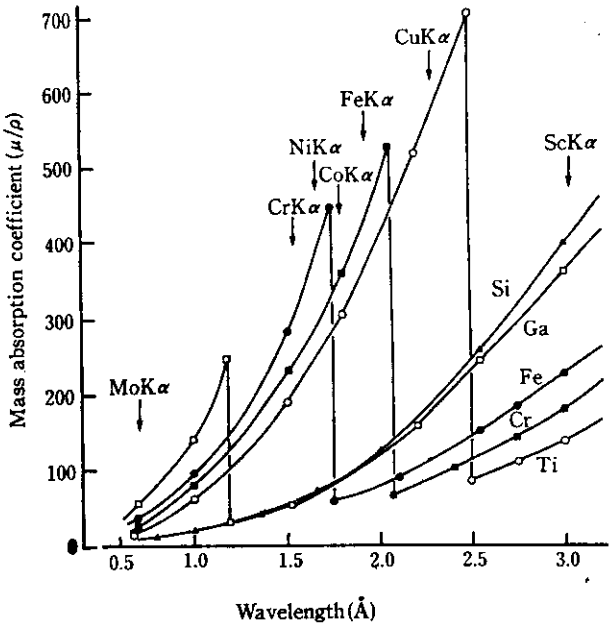

Fig. 4 Mass absorption coefficients of several elements

2.3 Features of Thin Film X-Ray Diffractometer

The goniometer portion of this diffractometer is schematically shown in **Fig. 5**. The X-ray penetration depth is reduced by a low angle incident beam. Furthermore, the detection of weak peaks of a thin film is made easy by providing a vacuum path. To increase signal-to-noise (S/N) rate and remove the white X-ray, a graphite flat crystal monochrometer and the non-focussing optical system are adopted. A specimen spinner is used as the specimen holder to reduce the strong texture effect, and a rotating anode (18 kW) is used as the X-ray source in order to increase intensity. Software capable of a maximum of 99 measurements can be used to raise the S/N rate of weak peaks.

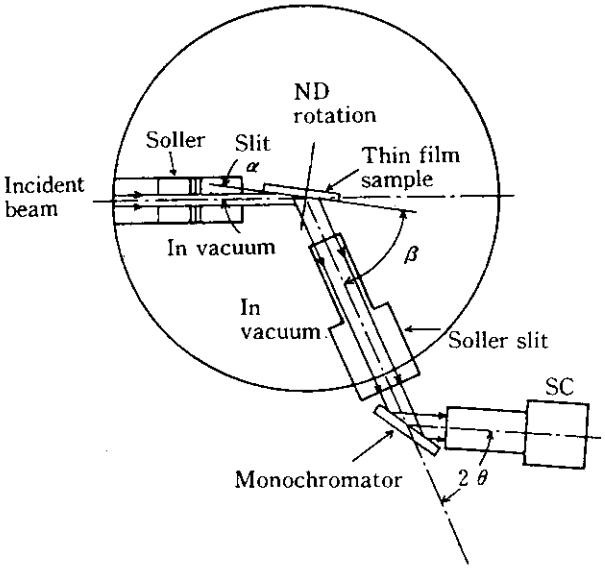

Fig. 5 Principle of the thin film goniometer (Rigaku 2655A1)

3 Examination of Diffractometer

3.1 Measurement Conditions

The measurement conditions are:

X-ray target : Cu
Tube voltage : 55 kV
Tube current : 250–280 mA
DS : 0.20 mm
SS : 5–6 mm
Scanning speed : 4°/min
Sampling step : 0.02°
Incident angle : 1.5–2.0°
X-ray pass : In vacuum (10^{-2} Torr~)

3.2 Comparison of Measurements in Air and Vacuum

It is difficult to analyze a substance when the film to be measured is too thin to obtain peaks or when the peaks are too weak. To improve this difficulty in analysis, a vacuum pass line is provided in the X-ray pass; the sealing material for the vacuum pass line was examined. An oxide film of AISI 430 was used as the specimen.

Figure 6 shows changes in the peak intensity of $FeCr_2O_4$ and Cr_2O_3 measured with the atmosphere and sealing material varied.

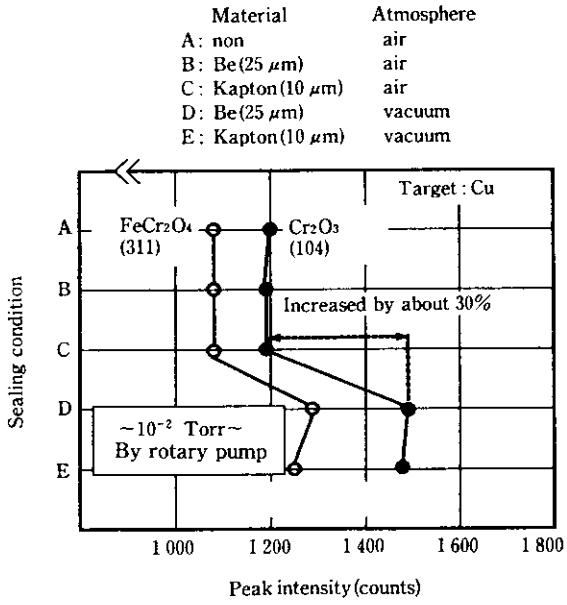

Fig. 6 Comparison of peak intensities between mesurement in air and that in vacuum

The measurement conditions A, B and C are those in the air; there is no difference in the peak intensity under these conditions. Under the conditions D and E, measurement was made in a vacuum (10^{-2} Torr~); four sheets of Be sealing foil (25 μm) were used in the former case, and four sheets of Kapton sealing foil (10 μm) in the latter. As is apparent from Fig. 6, the peak intensity obtained in a vacuum is about 30% higher than in the air. The increase in intensity is a little larger with the Be foil than with the Kapton foil. In view of the foregoing, the following measurement is made using this diffractometer under the conditions D.

3.3 Comparison between θ-2θ Method and TFXD Method

Figure 7 shows X-ray diffraction spectra of thin Si films deposited on glass plates to a thickness of tens of nm, which were measured according to the ordinary θ-2θ method and the TFXD method ($\alpha = 2°$). The measurements were made under the same conditions of voltage, current and slit. With this diffractometer, peaks incapable of being detected according to the θ-2θ method were clearly recognized. It was found from the Si (111), (220) and (311) peaks that the substance is crystallized, not amorphous. The TFXD method provides a remarkably improved film detection capacity.

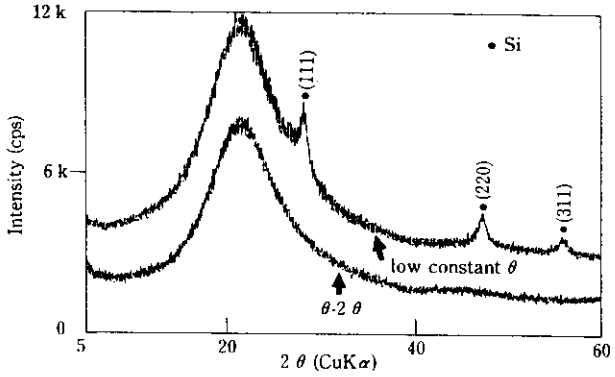

Fig. 7 X-ray diffraction spectra of Si thin films deposited on glass plates

3.4 Limit to Thin Film Measurement by TFXD

Figure 8 shows diffraction patterns of thin Fe films with various thicknesses deposited on glass plates. Because of the difficulty anticipated in detection, ten cumulative measurements were made in all of the specimens. No diffraction line of α-Fe was recognized in the usual θ-2θ measurement.

In specimen A, which is a thin α-Fe film a little thicker than 10 nm, a (110) peak is easily recognized. As with specimen A, a (110) peak is recognized in specimen B which is a thin film with a thickness of less than

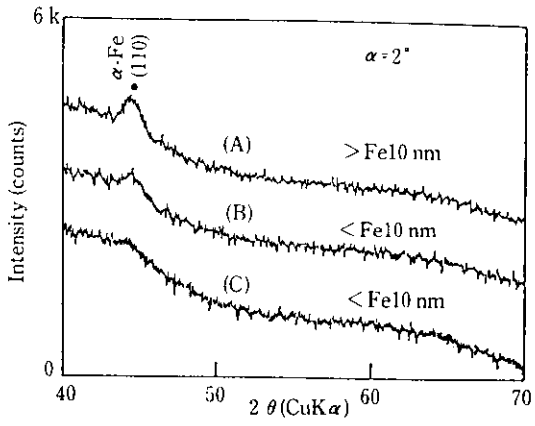

Fig. 8 XRD patterns of Fe thin films deposited on glass plates obtained by the thin film goniometer

10 nm. A (110) peak is slightly noted in film C that is thinner than specimen B. However, a (110) peak was not recognized in films thinner than specimen C.

A crystallized thin film of less than 10 nm can be recognized according to the TFXD method, although there may be a difference depending on the substance constituting the thin film and the X-ray source used. It is expected that this method will be very effective in the crystal structure analysis of the outermost material.

4 Examples of Application

4.1 Oxide Layers on AISI 430 Stainless Steel Sheet and Their Dissolution

The crystal structure of oxide layers formed on the surface of an AISI 430 stainless steel sheet during annealing was clarified, and the electrolysis conditions for removing oxide layers and the dissolution property of the oxide layers were examined. **Figure 9** shows the X-ray diffraction spectra of oxide layers formed on the surface of an AISI 430 stainless steel sheet annealed under various temperatures. There are two types of oxide layers: $FeCr_2O_4$ or Fe_3O_4 and $(FeCr)_2O_3$ or Cr_2O_3. Therefore, the coexistence of $FeCr_2O_4$ and Cr_2O_3 is here recognized. Next, **Figure 10** shows coulombs for dissolution (C/dm^2) and peak intensities of main diffraction lines of residual oxide films with respect to the dissolution property of surface oxide layers formed under the same annealing conditions. For both $FeCr_2O_4$ and Cr_2O_3, about 50% of the oxide film formed during annealing is removed at 25 C/dm^2. At 125 C/dm^2, about 90% of the oxide film dissolves. At 200 C/dm^2, 97% to 99% of the oxide film is removed. Also, it is apparent that the peak intensity of α-Fe in the steel sheet increases with decreasing amount of oxide film.

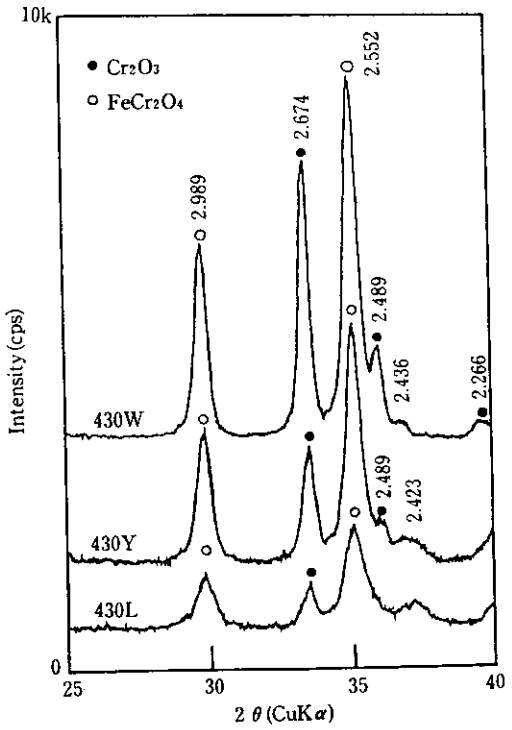

Fig. 9 X-ray diffraction spectra of annealed 430 stainless steels

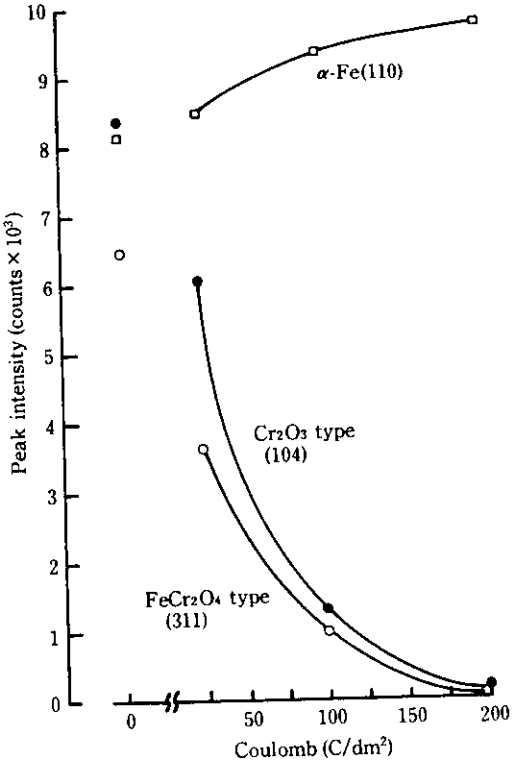

Fig. 10 Peak intensity changes with coulombs for dissolution of oxide films

4.2 Oxide Layers on Bright-Annealed AISI 304 Stainless Steel Sheet

Some of AISI 304 stainless steel sheets are bright-annealed in an inert gas after cold rolling to increase brightness depending on applications. In these bright-annealed steel sheets, the formation of oxide films is greatly influenced by the atmosphere in the annealing furnace. Substances formed on the surface of a bright-annealed steel sheet were identified at the various dew points in the furnace and the relationship between these substances and dew point was investigated. **Figure 11** shows X-ray diffraction patterns of thin film oxide layers formed on the surfaces of an as-cold-rolled steel sheet and bright-annealed steel sheets with the dew point in the annealing furnace varied appropriately between −58°C and −35°C. Although $FeCr_2O_4$ (311) is slightly recognized even in the cold-rolled steel sheet before bright annealing, the formation of oxide films does not change up to the dew point of −40°C. When the dew point rises to −38°C and −35°C, however, $FeCr_2O_4$ (311) and (220) are easily recognized and this shows that the formation of oxide films proceeds rapidly. No Cr_2O_3 oxide film is formed. The relationship between the peak intensity of diffraction line and the dew point is shown in **Fig. 12**. Although the $FeCr_2O_4$ oxide film does not increase at dew point temperatures below −40°C, it increases abruptly when the dew point is higher than −40°C. The formation of oxide films is greatly influenced by the dew point in the furnace, and an exact dew point control is currently conducted.

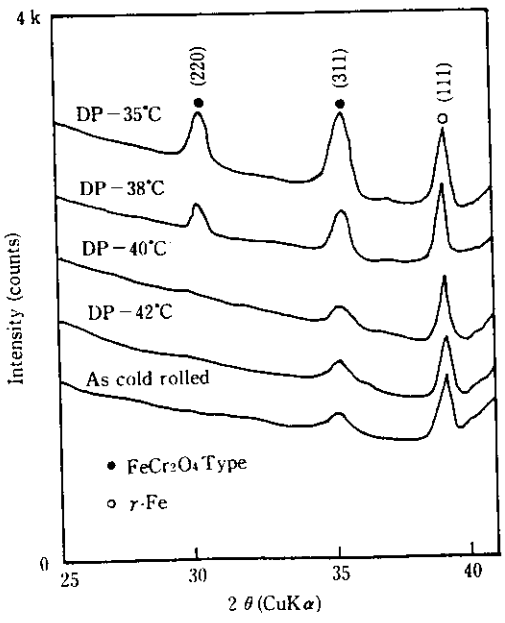

Fig. 11 X-ray diffraction spectra of 304 stainless steels bright annealed with different dew point temperatures

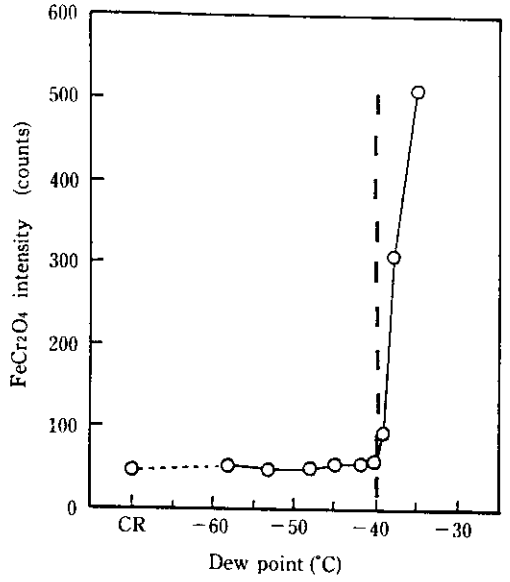

Fig. 12 Diffraction intensities of $FeCr_2O_4$ layer depending on dew point temperatures

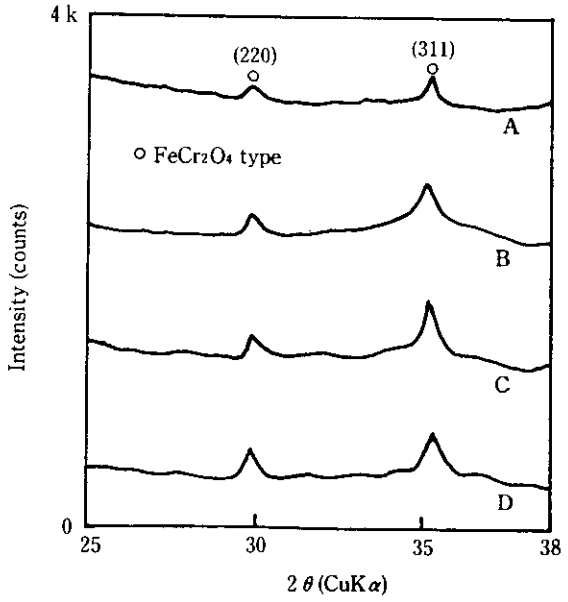

Fig. 13 Thin film diffraction spectra of films on 304 stainless steels

4.3 Crystal Structure of Electrochemically Colored Stainless Steel Sheet

The INCO process[8] prevails as an electrochemical coloring process for stainless steel sheets. This process involves the coloring of the sheet with a chromium sulfate solution and the hardening of the colored film. Naturally, the thin oxide film formed cannot be measured with the θ-2θ method. X-ray diffraction patterns of thin films formed in the INCO process are shown in **Fig. 13**. Specimen A is a bright-annealed steel sheet before coloring. Specimen B is a colored batch-annealed steel sheet without hardening. Specimens C and D are colored steel sheets hardened under different conditions for hardening the oxide film, such as solution temperature and current density. In specimen B, a broad diffraction curve which seems to be an amorphous substance is observed in addition to $FeCr_2O_4$. From specimens C and D, it became apparent that crystallization proceeds better when the film is hardened at a higher solution temperature and a higher current density and that the hardening conditions are related to film adhesion.

4.4 Crystallization of Fe-B-Si Amorphous Alloy

It is known that iron losses decrease in amorphous ribbons fabricated using a single roll technique if appropriate annealing is given. With heat treatment above crystallization temperatures, amorphous alloys crystallize and iron losses increase greatly; it is necessary, therefore, to control the annealing temperature carefully,[9] although this crystallization temperature changes depending on the atmosphere in the annealing furnace.

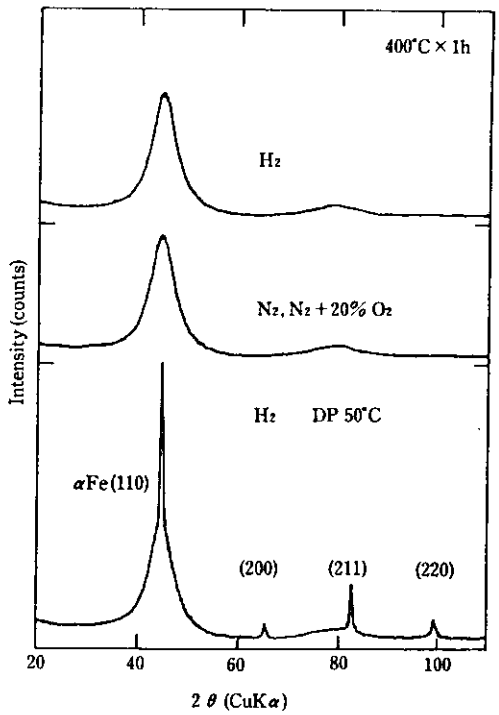

Fig. 14 X-ray diffraction spectra of $Fe_{78}B_{13}Si_9$ amorphous ribbons annealed in the different atmospheres

Figure 14 shows X-ray diffraction spectra of thin films on $Fe_{78}B_{13}Si_9$ ribbons annealed at a constant annealing temperature (400°C) for 1 h in different furnace atmospheres. Although crystallization does not occur in a ribbon annealed in a dry H_2 gas or a ribbon annealed in a

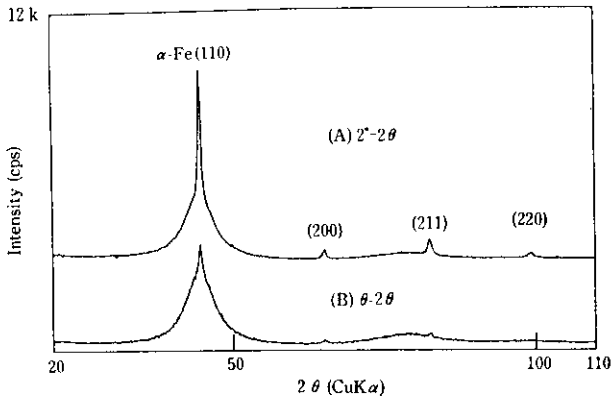

Fig. 15 X-ray diffraction spectra measured by (A) thin film goniometer and (B) conventional θ-2θ goniometer

dry $N_2 + O_2$ gas atmosphere, an α-Fe peak is observed in a ribbon annealed in a wet H_2 gas atmosphere (DP: 50°C), showing that crystallization in the ribbon is related to the iron loss increase.

X-ray diffraction spectra of a ribbon with partial crystallization were measured according to the conventional θ-2θ method and the TFXD method ($\alpha = 2°$) as shown in **Fig. 15**. In the spectrum A obtained with the TFXD method, crystallization has occurred relatively at random. In the spectrum B obtained with the θ-2θ, the peak is weak in a diffraction line at a high angle (2θ) and (220) peak is not observed, suggesting that crystallization occurs from the surface layer because the X-ray penetration depth is several times deeper in the conventional θ-2θ method than in the TFXD method and increases with increasing angle. The same was also confirmed from the observation of the section of the ribbon.

5 Conclusions

Kawasaki Steel's X-ray diffractometer with a vacuum pass line for the measurement of thin films formed on the surface of a material was applied to steel sheets, and the following results were obtained:

(1) Compared with the measurement in the air, the diffraction X-ray intensity was increased by about 30% by providing a vacuum pass line.

(2) Thin Si films deposited on glass plates beyond the detecting capacity of the θ-2θ method were easily recognized.

(3) α-Fe of thin films below 10 nm vacuum-deposited on glass plates was recognized.

(4) $FeCr_2O_4$ and Cr_2O_4 coexist in an oxide film formed on an AISI 304 stainless steel sheet.

(5) The oxide film formed on an AISI 430 stainless steel sheet can be removed 97% to 99% at 200 C/dm^2.

(6) The oxide film formed by bright annealing on an AISI 304 stainless steel sheet is only $FeCr_2O_4$, increasing markedly when the dew point in the furnace is higher than −40°C.

(7) The electrochemically colored film formed in the INCO process is $FeCr_2O_4$. The crystallization of this film differs depending on the solution temperature and current density.

(8) Fe-B-Si amorphous alloys show different crystallization tendencies depending on the atmosphere in the annealing furnace. Crystallization occurs from the surface layer.

The authors wish to thank the people of Rigaku Corporation for their cooperation in the fabrication of the vacuum pass line, which is one of the features of this diffractometer.

References

1) M. Katayama and M. Shimizu: *Tetsu-to-Hagané*, 72(1986)5, S418
2) M. Shimizu and M. Katayama: *Trans. ISIJ*, 27(1987)3, 239
3) M. Katayama, M. Shimizu, and T. Maeda: Proc. of the 24th Conference on X-ray and Material strength, (1987), December, 96
4) M. Katayama and M. Shimizu: Advances in X-ray Chemical Analysis, ed. by Japan Soc. for Analytical Chemistry, 19(1988), 281, [AGNE Publishing Ltd.]
5) H. S. Peiser, H. P. Rooksby, and A. J. C. Wilson: "X-ray Diffraction by Polycrystalline Materials", Inst. Phys., London, (1955), 159
6) Y. Kobayashi and M. Yoshimatsu: Advances in X-ray Chemical Analysis, ed. by Japan Soc. for Analytical Chemistry, 7(1975), 49, [AGNE Publishing Ltd.]
7) B. D. Cullity: "Elements of X-ray Diffraction", (1956), [Addison-Wesley]
8) H. Takamura: *The Stainless* (Japanese), 31(1967)4, 1
9) N. Morito, T. Maeda, T. Suzuki, T. Yamashita: *J. Jpn. Inst. Met.*, 52(1988)4, 420